Aberrant patterns of H3K4 and H3K27 histone lysine methylation occur across subgroups in medulloblastoma

Adrian M. Dubuc,
Division of Neurosurgery, Arthur & Sonia Labatt Brain, Tumour Research Centre, The Hospital for Sick Children, Toronto, ON, Canada. Program in Developmental & Stem Cell Biology, The Hospital for Sick Children, 555 University Avenue, Toronto, ON, Canada. Department of Laboratory Medicine & Pathobiology, University of Toronto, Toronto, ON, Canada

Marc Remke,
Division of Neurosurgery, Arthur & Sonia Labatt Brain, Tumour Research Centre, The Hospital for Sick Children, Toronto, ON, Canada. Program in Developmental & Stem Cell Biology, The Hospital for Sick Children, 555 University Avenue, Toronto, ON, Canada. Department of Laboratory Medicine & Pathobiology, University of Toronto, Toronto, ON, Canada

Andrey Korshunov,
CCU Neuropathology, German Cancer Research Centre (DKFZ), Heidelberg, Germany. Department of Neuropathology, University of Heidelberg, Heidelberg, Germany. Division of Pediatric Neurooncology, German Cancer Research Centre (DKFZ), Heidelberg, Germany

Paul A. Northcott,
Division of Pediatric Neurooncology, German Cancer Research Centre (DKFZ), Heidelberg, Germany

Shing H. Zhan,
Genome Sciences Centre, British Columbia Cancer Agency, Vancouver, BC, Canada

Maria Mendez-Lago,
Genome Sciences Centre, British Columbia Cancer Agency, Vancouver, BC, Canada

Marcel Kool,
Division of Pediatric Neurooncology, German Cancer Research Centre (DKFZ), Heidelberg, Germany

David T. W. Jones,
Division of Pediatric Neurooncology, German Cancer Research Centre (DKFZ), Heidelberg, Germany

Alexander Unterberger,
Division of Neurosurgery, Arthur & Sonia Labatt Brain, Tumour Research Centre, The Hospital for Sick Children, Toronto, ON, Canada. Program in Developmental & Stem Cell Biology, The Hospital for Sick Children, 555 University Avenue, Toronto, ON, Canada

A. Sorana Morrissy,
Division of Neurosurgery, Arthur & Sonia Labatt Brain, Tumour Research Centre, The Hospital for Sick Children, Toronto, ON, Canada. Program in Developmental & Stem Cell Biology, The Hospital for Sick Children, 555 University Avenue, Toronto, ON, Canada

Correspondence to: Michael D. Taylor, mdtaylor@sickkids.ca.

David Shih,

Division of Neurosurgery, Arthur & Sonia Labatt Brain, Tumour Research Centre, The Hospital for Sick Children, Toronto, ON, Canada. Program in Developmental & Stem Cell Biology, The Hospital for Sick Children, 555 University Avenue, Toronto, ON, Canada. Department of Laboratory Medicine & Pathobiology, University of Toronto, Toronto, ON, Canada

John Peacock,

Division of Neurosurgery, Arthur & Sonia Labatt Brain, Tumour Research Centre, The Hospital for Sick Children, Toronto, ON, Canada. Program in Developmental & Stem Cell Biology, The Hospital for Sick Children, 555 University Avenue, Toronto, ON, Canada. Department of Laboratory Medicine & Pathobiology, University of Toronto, Toronto, ON, Canada

Vijay Ramaswamy,

Division of Neurosurgery, Arthur & Sonia Labatt Brain, Tumour Research Centre, The Hospital for Sick Children, Toronto, ON, Canada. Program in Developmental & Stem Cell Biology, The Hospital for Sick Children, 555 University Avenue, Toronto, ON, Canada. Department of Laboratory Medicine & Pathobiology, University of Toronto, Toronto, ON, Canada

Adi Rolider,

Division of Neurosurgery, Arthur & Sonia Labatt Brain, Tumour Research Centre, The Hospital for Sick Children, Toronto, ON, Canada. Program in Developmental & Stem Cell Biology, The Hospital for Sick Children, 555 University Avenue, Toronto, ON, Canada

Xin Wang,

Division of Neurosurgery, Arthur & Sonia Labatt Brain, Tumour Research Centre, The Hospital for Sick Children, Toronto, ON, Canada. Program in Developmental & Stem Cell Biology, The Hospital for Sick Children, 555 University Avenue, Toronto, ON, Canada. Department of Laboratory Medicine & Pathobiology, University of Toronto, Toronto, ON, Canada

Hendrik Witt,

Division of Pediatric Neurooncology, German Cancer Research Centre (DKFZ), Heidelberg, Germany

Thomas Hielscher,

Division of Pediatric Neurooncology, German Cancer Research Centre (DKFZ), Heidelberg, Germany

Cynthia Hawkins,

Division of Neurosurgery, Arthur & Sonia Labatt Brain, Tumour Research Centre, The Hospital for Sick Children, Toronto, ON, Canada. Program in Developmental & Stem Cell Biology, The Hospital for Sick Children, 555 University Avenue, Toronto, ON, Canada. Department of Laboratory Medicine & Pathobiology, University of Toronto, Toronto, ON, Canada

Rajeev Vibhakar,

Department of Pediatrics, The Children's Hospital and University of Colorado, Anschutz Medical Campus, Colorado, USA

Sidney Croul,

Department of Pathology, University Health Network, University of Toronto, Toronto, ON, Canada

James T. Rutka,

Division of Neurosurgery, Arthur & Sonia Labatt Brain, Tumour Research Centre, The Hospital for Sick Children, Toronto, ON, Canada. Department of Laboratory Medicine & Pathobiology, University of Toronto, Toronto, ON, Canada

William A. Weiss,

Helen Diller Family Comprehensive Cancer Centre, University of California, San Francisco, CA, USA

Steven J. M. Jones,
Genome Sciences Centre, British Columbia Cancer Agency, Vancouver, BC, Canada

Charles G. Eberhart,
Department of Pathology, Johns Hopkins University, Baltimore, MD, USA

Marco A. Marra,
Genome Sciences Centre, British Columbia Cancer Agency, Vancouver, BC, Canada

Stefan M. Pfister, and
Division of Pediatric Neurooncology, German Cancer Research Centre (DKFZ), Heidelberg,
Germany

Michael D. Taylor
Division of Neurosurgery, Arthur & Sonia Labatt Brain, Tumour Research Centre, The Hospital for
Sick Children, Toronto, ON, Canada. Program in Developmental & Stem Cell Biology, The
Hospital for Sick Children, 555 University Avenue, Toronto, ON, Canada. Department of
Laboratory Medicine & Pathobiology, University of Toronto, Toronto, ON, Canada

Michael D. Taylor: mdtaylor@sickkids.ca

Abstract

Recent sequencing efforts have described the mutational landscape of the pediatric brain tumor medulloblastoma. Although *MLL2* is among the most frequent somatic single nucleotide variants (SNV), the clinical and biological significance of these mutations remains uncharacterized. Through targeted re-sequencing, we identified mutations of *MLL2* in 8 % (14/175) of MBs, the majority of which were loss of function. Notably, we also report mutations affecting the MLL2-binding partner *KDM6A*, in 4 % (7/175) of tumors. While *MLL2* mutations were independent of age, gender, histological subtype, M-stage or molecular subgroup, *KDM6A* mutations were most commonly identified in Group 4 MBs, and were mutually exclusive with *MLL2* mutations. Immunohistochemical staining for H3K4me3 and H3K27me3, the chromatin effectors of MLL2 and KDM6A activity, respectively, demonstrated alterations of the histone code in 24 % (53/220) of MBs across all subgroups. Correlating these MLL2-and KDM6A-driven histone marks with prognosis, we identified populations of MB with improved (K4+/K27−) and dismal (K4−/K27−) outcomes, observed primarily within Group 3 and 4 MBs. Group 3 and 4 MBs demonstrate somatic copy number aberrations, and transcriptional profiles that converge on modifiers of H3K27-methylation (*EZH2*, *KDM6A*, *KDM6B*), leading to silencing of PRC2-target genes. As PRC2-mediated aberrant methylation of H3K27 has recently been targeted for therapy in other diseases, it represents an actionable target for a substantial percentage of medulloblastoma patients with aggressive forms of the disease.

Keywords

Introduction

Medulloblastoma (MB) is the most common malignant pediatric brain tumor and an
emerging model for the integrative use of clinical and molecular features to improve patient
stratification [24]. Although 5-year survival rates for standard risk patients exceed 70 %,
many survivors suffer from radiotherapy-related neurocognitive side effects, highlighting
the need for targeted therapies [12]. Our contemporary understanding of MB has shifted
rather strikingly as large cohort studies have effectively dissected MB from a single disease
into four disparate molecular subgroups each with specific transcriptional, genomic and

clinical features [25]. While the copy number and transcriptional heterogeneity has been well described, characterization of the mutational landscape has only recently emerged [9, 19, 20].

The first genome-wide MB mutational screen, performed by Parsons et al. [17] identified *MLL2* as among the most frequent somatic mutation, occurring in 14 % (12/88) of sequenced tumors. While this finding supported initial reports of copy number-driven alterations of the histone code in the pathogenesis of MB [16], the clinical and molecular significance of the novel mutations were not described. Given the strong prognostic association between *CTNNB1* mutations and improved patient outcome [5] and the subgroup-dependent survival effect of *TP53* mutations [18], we investigated the role of mutations targeting *MLL2* and its binding partner *KDM6A* across a large cohort of MB patients to determine if there was an association with patient outcome.

MLL2 is the catalytic component of trithorax group (trxG) proteins, that methylate histone H3 tails at the fourth lysine position (H3K4me) and creating a transcriptionally permissive chromatin state [22]. KDM6A, also a trxG protein, binds MLL2, but acts as a H3K27-trimethylation (me3) demethylase [22]. TrxG proteins function in concert to activate gene expression, through the combinatorial accumulation of active H3K4me3 residues and the removal of H3K27me3 repressive marks. The actions of TrxG proteins are opposed by Polycomb (PcG) group proteins, composed of two subunits (PRC1 and PRC2), which function antagonistically to repress gene transcription through accumulation of H3K27me3 marks [23].

Recent studies have demonstrated that the progenitor state is maintained through bivalent chromatin domains, a balancing act of inhibitory (H3K27me) and activating (H3K4me) chromatin marks at promoters of cell determinant factors, including many neural genes [23] (Fig. 5a). Differentiation is induced in part through shifts in the chromatin state of promoters, allowing pro-differentiation genes to be expressed [23]. In tumor cells, the chromatin state is hijacked through up-regulation of a number of PcG genes and loss of TrxG remodeling genes, resulting in inappropriate silencing of pro-differentiation genes [23]. These changes, which include *MLL2* and *KDM6A* mutations, identified in numerous cancers [8, 14] suggest that aberrations of the histone code are a common mechanism in the initiation, maintenance or progression of cancer. The development of pharmacological inhibitors of PcG-gene components, including the EZH2 inhibitors 3-Deazane-planocin (DZNep) [1] and GSK126 [13], has demonstrated promising preliminary results inhibiting cancer-induced H3K27me3-repressive marks, and sensitizing cells to apoptotic agents [1]. Given the relatively high frequency of *MLL2* mutations in MB, we focused our efforts on characterizing the prognostic use and biological effect of somatic mutations affecting modifiers of the histone code, and global changes in the chromatin state mediated by H3K4me3 and H3K27me3 patterns across a combined total of 463 tumors.

Materials and methods

Patient characteristics

Medulloblastomas derived from 175 (*n* = 175) patients where sufficient DNA or tissue was available and where robust clinical details were available were included in our sequencing cohort, accurately reflecting the known demographics, molecular subgroups, and histology of this disease. Annotated clinical and histological data for sequenced tumors and TMAs (JHU, *n* = 50; DKFZ, *n* = 238) are outlined in Supplementary Table 1.

MLL2 and *KDM6A* sequencing

MLL2 and *KDM6A* were sequenced using an exon-capture workflow across 175 tumors which form the discovery sequencing cohort. In brief, capture probes designed against coding sequences were used to pull down sonicated genomic DNA. Barcoding and sequence adaptors were ligated and sequencing was performed using Illumina GAIIX sequencer. Following alignment to the reference genome (Hg18) using BWA alignment software, single nucleotide variants (SNVs) were detected using SNVmix2 (pAB + pBB ≥0.99) and insertions/deletions (INDELs) were detected using SamTools (Consensus quality ≥50). Predicted SNVs were filtered through BC Genome Sciences Centre (GSC) in-house database of normal genomes, which is used to store and process human variation [6]. The database contains variation data from genomes sequenced at BC GSC, the 1,000 Genomes Project, dbSNP132 as well as other publically available genomes. Filtered SNVs were visually inspected using integrative genomic viewer (IGV) and final curated mutations were validated using Sanger sequencing. The validation cohort was composed of four previously published series: Jones et al. [9], Parsons et al. [17], Pugh et al. [19] and Robinson et al. [20] totaling 398 primary medulloblastomas.

Immunohistochemistry

TMAs obtained from the German Cancer Research Centre (DKFZ) and Johns Hopkin's University (JHU) were stained using antibodies directed towards H3K4me3 (1:1,000 CIT, No. 9751; Cell Signaling Technology, Danvers, MA) H3K27me3 (1:10,000 CIT and PEP 1 min, No. 07-449, Millipore, Billerica, MA) and MLL2 (1:1,000, HPA035977, Sigma Aldrich, St. Louis, MO). Stained TMAs were scored in two semi-quantitative manners (negative, positive or super-negative, weak positive, positive) by two independent reviewers (A.K. and A.M.D.) who were blinded to clinical and molecular patient variables.

Copy number and expression analysis

Single nucleotide polymorphisms (SNP) 100 K and 500 K arrays were processed on a series of 201 primary medulloblastomas as previously described [16]. Similarly, Affymetrix Exon 1.0ST arrays were used to analyze the transcriptome of 103 primary tumors. Array analysis and molecular subgroup assignment were performed as previously described [15]. Both expression sets were previously deposited in GEO under GSE14437 and GSE21140.

Results

MLL2 mutations occur in a subgroup-independent manner

We performed targeted sequencing (Supplementary Fig. S1) on a clinically annotated discovery cohort of 175 MBs, reflecting the spectrum of demographics, molecular subgroups, and histological subtypes of the disease (Supplementary Table S1) [11]. We verified our results using a validation cohort of 398 previously sequenced medulloblastomas from four independent centers [9, 17, 19, 20]. In our discovery series, eight percent (8 %, 14/175) of tumors harbored *MLL2* mutations independent of age or histological subtypes (Fig. 1a; Supplementary Table S2). No homozygous mutations were identified (Fig. 1b, Supplementary Fig. S2a) and 45 % (9/20) of those mutations detected disrupted the coding sequence through nonsense and frameshift mutations (Fig. 1c; Supplementary Table S2). While the mutation frequency (Fig. 1a) and zygosity (Fig. 1b) across our validation cohort supported our discovery cohort, there was a 22–35 % increase in the frequency of damaging mutations (Fig. 1c). *MLL2* mutations occurred in a similar frequency across non-WNT subgroups in our discovery cohort (Fig. 1d); however, there was considerable variability in the molecular distribution across the validation cohort, with an increased incidence of *MLL2* mutations in WNT tumors reported by Jones et al. [9], whereas studies by Pugh et al. [19]

and Robinson et al. [20] have a greater incidence of SHH *MLL2* mutations. Across the combined discovery and validation series ($n = 573$), the SHH subgroup has the highest total number of tumors with *MLL2* mutations ($n = 13$) and represents the only subgroup where >1 MLL2 mutation per tumor genome was identified (Supplementary Fig. S2c). No *MLL2* mutational hotspots exist and only a single recurrent mutation (1/53, R5501*) was identified across the combined cohort (Fig. 1e). *MLL2* mutational status, however, provided no prognostic or diagnostic utility (Supplementary Fig. S3a).

An expression analysis reveals that *MLL2* has a relatively lower expression in WNT and SHH tumors as compared with Group 3 and Group 4 medulloblastomas (Supplementary Fig. S2d) and MLL2-immunonegativity was a predictor of unfavorable outcome across non-WNT/non-SHH MBs ($P < 4.63E-2$; Fig. 1f). Inactivation of MLL2 appears to be restricted to the level of the nucleotide (i.e., mutational) as no copy number alterations (i.e., deletions, $1.5 < MLL2\ CN > 2.75$) were observed in a large cohort of primary tumors analyzed ($n = 201$) [16] (Supplementary Fig. S2e).

Genomic and mutational inactivation of *KDM6A* in Group 4 medulloblastomas

A previous characterization of copy number alterations in the medulloblastoma genome identified a focal deletion targeting *KDM6A* (0.5 %, 1/201) located on Xp11.3 (Fig. 2a). In addition, broad genetic loss of the X-chromosome frequently occurs in MB, targeting the inactive X-chromosome [10]. We examined the subgroup-specificity of this cytogenetic event, demonstrating a significant ($P < 4.00E-3$) enrichment in Group 4 MBs, affecting 22 % (8/36) of tumors (Fig. 2b). Given previous reports suggesting that both deletions and mutations lead to *KDM6A* inactivation [8], we pursued a targeting sequencing approach to identify the incidence and nature of *KDM6A* SNVs in medulloblastoma.

Our approach identified one additional *KDM6A* deletion (0.6 %, 1/175), spanning exons 5 through 13 (Fig. 2c), while somatic mutations were identified in 4 % (7/175) of MBs (Fig. 2d). *KDM6A* mutations were often homozygous (57 %, 4/7) (Fig. 2e) causing premature termination of the transcript (nonsense), or frameshift mutations in the majority of cases (86 %, 6/7) (Fig. 2f). No correlation was observed between *KDM6A* mutations and age, gender, histology, or M-stage (Supplementary Table S3) in the discovery cohort, results which were confirmed across the validation cohort. Interestingly, *KDM6A* mutations occur predominantly in Group 4 medulloblastomas (Fig. 1g), localized to the 3′ coding exons (Fig. 2h).

Deregulation of the histone code across multiple subgroups of medulloblastoma

MLL2 and *KDM6A* mutations were mutually exclusive ($P = 8.60E-6$) suggesting that the trxG-mediated histone code is affected in at least 12 % (21/175) of MBs within the discovery and 11 % (45/398) of the validation cohort based on our mutational analysis alone (Fig. 3a). A single tumor (1/66) across the combined cohorts was detected with mutations affecting both genes (Fig. 3a, right); however, the *MLL2* mutation present within this tumor was a missense (D5028Y) mutation that did not disrupt the coding sequence.

Modifications of chromatin state represent a recurrent and important theme in the pathogenesis of MB. Therefore, we evaluated immunostaining of H3K4me3 and H3K27me3, the chromatin effectors of *MLL2* and *KDM6A*, in two independent tumor cohorts (JHU, $n = 50$; DKFZ, $n = 238$). In both patient series, loss of H3K4me3 demonstrated a trend towards decreased survival (Supplementary Fig. S5a). By contrast, no clear trends were observed regarding H3K27me3 staining patterns across the two cohorts (Supplementary Fig. S5b). Given that trxG proteins function as a complex to increase transcriptionally active H3K4me3 marks while simultaneously removing H3K27me3

repressive marks, we overlaid these two histone modifications, where this information was available ($n = 220$).

While the majority of MBs stain positive for both H3K4me3 and H3K27me3 (K4+/K27+; 76 %, 167/220), a significant fraction of samples (24 %, 53/220) demonstrated isolated or combined loss of these chromatin marks (Fig. 3b). This deregulation of the normal histone code occurs across all molecular subgroups of MB. Importantly, there is a significant difference in overall survival of H3K4me3-positive/H3K27me3-negative (K4+/K27−) staining sections versus dual negative (K4−/K27−; $P < 7.60E−3$) or dual positive (K4+/K27+; $P < 3.37E−2$) samples (Fig. 3d). The improved outcome associated with K4+/K27− chromatin state appears to be driven by Group 3 and Group 4 MBs ($P < 7.20E−3$ versus dual positive; $P < 4.40E−3$ versus dual negative), as no survival differences associated with the chromatin state were observed in WNT or SHH MBs.

Identification of an H3K27me3-enriched (K27+) phenotype in Group 4 medulloblastomas

Given the mutational and genomic enrichment for *KDM6A* inactivation in Group 4 MBs, we examined the transcriptional and copy number status of other known modifiers of H3K27. *EZH2*, an H3K27-methyltransferase, has previously been reported as significantly over-expressed and amplified in Group 4 MBs [1]. In addition, *KDM6B*, an H3K27-demethylase, was previously reported as mutated (0.3 %, 1/398) in MBs [9, 17, 19, 20]. At the level of the genome, *EZH2* (chr7q36.1) and *KDM6B* (17p13.1) undergo frequent copy number alterations with chromosome 7 gains and single copy loss of chr17p occurring in 14 % (29/201) and 15 % (30/210) of tumors, respectively. These aberrations, in conjunction with the aforementioned loss of *KDM6A* (chrXp11.3), affect 31 % (62/201) of all MBs. A subgroup-specific analysis demonstrates a significant enrichment ($P < 2.87E−2$) in Group 3/Group 4 MBs, with 46 % (13/28) of Group 3 and 56 % (20/36) of Group 4 MBs tumors displaying one or multiple cytogenetic events converging on H3K27 modifiers (Fig. 4a). These cytogenetic alterations were concomitant with gene expression changes for both *EZH2* and *KDM6A* (Supplementary Fig. 6).

Correlation of *EZH2*, *KDM6A* and *KDM6B* expression demonstrates a strong H3K27me3-enrichment (K27+) phenotype (*EZH2*-high; *KDM6A*/*KDM6B*-low) exclusively in Group 3 (7 %, 2/27) and Group 4 tumors (11 %, 5/35) as compared with WNT (0/8) and SHH (0/33) subgroups (Fig. 4b, c). These findings were reproducible in an independent, non-overlapping MB dataset ($n = 187$), identifying a similar correlation between K27+ and Group 3 and Group 4 tumors (Fig. 4c, right). We examined the transcriptional consequences of the K27+ phenotype, by comparing K27+ versus non-enriched tumors. Molecular Signature Database (MsigDB) analysis revealed a significant over-representation of PRC2/H3K27me3 targets in genes demonstrating significant ($P < 0.05$) and differentially (>2-fold) expression across both transcriptome datasets (Fig. 4d). While the two transcriptome series have limited overlap in the genes commonly associated with the K27+ phenotype (Fig. 4e), the strong differential expression of common candidate markers suggest that diagnostic tools could be rapidly developed to identify populations of Group 3 and Group 4 MBs with a H3K27m3-enriched phenotype (Fig. 4f).

Discussion

Our investigation sought to characterize the clinical and biological characteristics of medulloblastomas with mutations affecting *MLL2* and/or its binding partner *KDM6A*. Our results demonstrate that *MLL2* mutations occur in 5–14 % of tumors independent of molecular subgroup or histological subtype. These mutations frequently ablate the enzymatic methyltransferase activity in one copy of *MLL2* through heterozygous frameshift and nonsense mutations. The combined discovery and validation cohort confirms a lack of

mutational hot spots and the heterozygous nature of *MLL2* mutations. Our results highlight that while *MLL2* mutations occur in a subgroup-independent manner, geographical variations in the mutation penetrance and subgroup-specificity exist. Specifically, *MLL2* mutations identified in European patients (profiled in the Jones et al. [9] study) were identified in a high percentage of WNT tumors and a much lower frequency of SHH tumors. These trends are reversed in North American patients where no *MLL2* mutations were identified in WNT tumors and a much higher incidence of SHH tumors. *MLL2* mutations provide no prognostic or diagnostic utility, however, MLL2-immunonegativity significantly associated with decreased overall survival in non-WNT, non-SHH medulloblastomas. The near absence (1/53) of homozygous *MLL2* mutations highlights a possible oncogenic dependence on the maintenance of H3K4-methylation in tumor cells. Given the established role of MLL2 as a critical requirement for oocyte survival and H3K4me3 maintenance [2, 7], our results suggest that further silencing of *MLL2* may represent a synthetic lethal therapeutic avenue in subsets of MBs with *MLL2* mutations. While this therapeutic approach would offer a tumor-specific effect, based on the remaining active copy of *MLL2* in normal cells, the lack of mutational hot spots and size of the *MLL2* coding sequence makes this approach particularly challenging.

Mutational analysis of the MLL2-binding partner *KDM6A* revealed mutations in 4–8 % of sequenced tumors, predominantly in Group 4 medulloblastomas. The vast majority (>80 %) of mutations disrupted the coding sequence and many homozygous mutations were identified. *KDM6A* is also affected at a copy number level via intragenic deletions or loss of the entire X-chromosome, which is most prominently observed in Group 4 tumors. Our results suggest that *KDM6A* inactivation can occur through multiple, independent cancer-specific changes including mutations and copy number alterations, and are particularly prevalent in Group 4 medulloblastomas.

MLL2 and *KDM6A* mutations principally occurred in a mutually exclusive pattern suggesting a minimum of 11–12 % of medulloblastomas have defects in the trxG-mediated histone code. Immunohistochemical analyses of H3K4me3 (K4+) and H3K27me3 (K27+) identifies a significant fraction of tumors with deregulation of Trithorax (trxG) and Polycomb (PcG) suggesting that additional molecular aberrations, beyond *MLL2* and *KDM6A* mutations, likely induce deregulation of the histone code in medulloblastoma. Overlaying these histone marks identified populations of tumors with improved (K4+/K27−) and dismal (K4−/K27−) outcomes. In future studies, the use of chromatin-immunoprecipitation (ChIP) will permit the identification of cancer-induced changes to the histone code at specific promoters, and may provide a greater understanding of the transcriptional consequences of epigenetic modifications. Our findings suggest that chromatin deregulation occurs across all medulloblastoma subgroups, and therefore might represent an attractive target for therapy in a substantial percentage of medulloblastoma patients.

In addition, Group 3 and Group 4 medulloblastomas display distinct changes in their chromatin state, through the acquisition of mutational, copy number and transcriptional aberrations resulting in a net H3K27me3-enriched (K27+) phenotype with consequent down-regulation of PRC2-target genes. These tumors may be identified using surrogate markers of PRC2 activity based on gene expression of *NMU*, *SST* and *CA10*, respectively. Conservatively, K27+ tumors affect a minimum 10 % of Group 4 medulloblastomas, in which *EZH2* is up-regulated with concomitant down-regulation of both *KDM6A* and *KDM6B*. However, 57 % of Group 4 tumors demonstrate EZH2 up-regulation with decreased expression of either demethylase (*KDM6A* or *KDM6B*). Following the identification of the four distinct medulloblastoma molecular subgroups, much effort has been placed on elucidating subgroup-specific and less toxic therapeutics. While this

approach has been promising for SHH tumors [21], and less crucial for WNT tumors, where long-term survival currently exceeds 90 % [25], the outcome for Group 3 and Group 4 tumors remains bleak. Thus, the need for targetable pathways is pressing. Epigenetic modifiers have considerable promise in the treatment of medulloblastoma, suppressing the initiation of tumorigenesis in mouse models of this disease [4], and resulting in enhanced apoptosis via pharmacological targeting of EZH2 activity in MB cell lines [1]. Given the reported success of histone deacetylase inhibitor (HDACi) in preclinical setting [3], our results suggest that histone modifying therapies may represent a promising therapeutic avenue for the treatment of aggressive medulloblastoma subgroups.

Supplementary Material

Refer to Web version on PubMed Central for supplementary material.

Acknowledgments

References

1. Alimova I, Venkataraman S, Harris P, Marquez VE, Northcott PA. Targeting the enhancer of zeste homologue 2 in medulloblastoma. Int J Cancer. 201210.1002/ijc.27455

2. Andreu-Vieyra CV, Chen R, Agno JE, Glaser S, Anastassiadis K, et al. MLL2 is required in oocytes for bulk histone 3 lysine 4 trimethylation and transcriptional silencing. PLoS Biol. 2010; 8(8):e1000453. [PubMed: 20808952]

3. Bots M, Johnstone RW. Rational combinations using HDAC inhibitors. Clin Cancer Res. 2009; 15(12):3970–3977. [PubMed: 19509171]

4. Ecke I, Petry F, Rosenberger A, Tauber S, Monkemeyer S, et al. Antitumor effects of a combined 5-aza-2′ deoxycytidine and valproic acid treatment on rhabdomyosarcoma and medulloblastoma in Ptch mutant mice. Cancer Res. 2009; 69(3):887–895. [PubMed: 19155313]

5. Ellison DW, Onilude OE, Lindsey JC, Lusher ME, Weston CL, et al. beta-Catenin status predicts a favorable outcome in childhood medulloblastoma: the United Kingdom Children's Cancer Study Group Brain Tumour Committee. J Clin Oncol. 2005; 23(31):7951–7957. [PubMed: 16258095]

6. Fejes AP, Khodabakhshi AH, Birol I, Jones SJ. Human variation database: an open-source database template for genomic discovery. Bioinformatics. 2011; 27(8):1155–1156. [PubMed: 21367872]

7. Glaser S, Schaft J, Lubitz S, Vintersten K, van der Hoeven F, et al. Multiple epigenetic maintenance factors implicated by the loss of Mll2 in mouse development. Development. 2006; 133(8):1423–1432. [PubMed: 16540515]

8. van Haaften G, Dalgliesh GH, Davies H, Chen L, Bignell G, et al. Somatic mutations of the histone H3K27 demethylase gene UTX in human cancer. Nat Genet. 2009; 41(5):521–523. [PubMed: 19330029]

9. Jones DT, Jager N, Kool M, Zichner T, Hutter B, et al. Dissecting the genomic complexity underlying medulloblastoma. Nature. 2012; 488(7409):100–105. [PubMed: 22832583]

10. Kool M, Koster J, Bunt J, Hasselt NE, Lakeman A, et al. Integrated genomics identifies five medulloblastoma subtypes with distinct genetic profiles, pathway signatures and clinico-pathological features. PloS One. 2008; 3(8):e3088. [PubMed: 18769486]

11. Kool M, Korshunov A, Remke M, Jones DT, Schlanstein M, et al. Molecular subgroups of medulloblastoma: an international meta-analysis of transcriptome, genetic aberrations, and clinical data of WNT, SHH, Group 3, and Group 4 medulloblastomas. Acta Neuropathol. 2012; 123(4): 473–484. [PubMed: 22358457]

12. Lafay-Cousin L, Bouffet E, Hawkins C, Amid A, Huang A, et al. Impact of radiation avoidance on survival and neurocognitive outcome in infant medulloblastoma. Curr Oncol. 2009; 16(6):21–28. [PubMed: 20016743]

13. McCabe MT, Ott HM, Ganji G, Korenchuk S, Thompson C, et al. EZH2 inhibition as a therapeutic strategy for lymphoma with EZH2-activating mutations. Nature. 201210.1038/nature 11606

14. Morin RD, Mendez-Lago M, Mungall AJ, Goya R, Mungall KL, et al. Frequent mutation of histone-modifying genes in non-Hodgkin lymphoma. Nature. 2011; 476(7360):298–303. [PubMed: 21796119]

15. Northcott PA, Korshunov A, Witt H, Hielscher T, Eberhart CG, et al. Medulloblastoma comprises four distinct molecular variants. J Clin Oncol. 2011; 29(11):1408–1414. [PubMed: 20823417]

16. Northcott PA, Nakahara Y, Wu X, Feuk L, Ellison DW, et al. Multiple recurrent genetic events converge on control of histone lysine methylation in medulloblastoma. Nat Genet. 2009; 41(4): 465–472. [PubMed: 19270706]

17. Parsons DW, Li M, Zhang X, Jones S, Leary RJ, et al. The genetic landscape of the childhood cancer medulloblastoma. Science. 2011; 331(6016):435–439. [PubMed: 21163964]

18. Pfaff E, Remke M, Sturm D, Benner A, Witt H, et al. TP53 mutation is frequently associated with CTNNB1 mutation or MYCN amplification and is compatible with long-term survival in medulloblastoma. J Clin Oncol. 2010; 28(35):5188–5196. [PubMed: 21060032]

19. Pugh TJ, Weeraratne SD, Archer TC, Pomeranz Krummel DA, Auclair D, et al. Medulloblastoma exome sequencing uncovers subtype-specific somatic mutations. Nature. 2012; 488(7409):106–110. [PubMed: 22820256]

20. Robinson G, Parker M, Kranenburg TA, Lu C, Chen X, et al. Novel mutations target distinct subgroups of medulloblastoma. Nature. 2012; 488(7409):43–48. [PubMed: 22722829]

21. Rudin CM, Hann CL, Laterra J, Yauch RL, Callahan CA, et al. Treatment of medulloblastoma with hedgehog pathway inhibitor GDC-0449. N Engl J Med. 2009; 361(12):1173–1178. [PubMed: 19726761]

22. Schuettengruber B, Chourrout D, Vervoort M, Leblanc B, Cavalli G. Genome regulation by polycomb and trithorax proteins. Cell. 2007; 128(4):735–745. [PubMed: 17320510]

23. Schuettengruber B, Martinez AM, Iovino N, Cavalli G. Trithorax group proteins: switching genes on and keeping them active. Nat Rev Mol Cell Biol. 2011; 12(12):799–814. [PubMed: 22108599]

24. Tamayo P, Cho YJ, Tsherniak A, Greulich H, Ambrogio L, et al. Predicting relapse in patients with medulloblastoma by integrating evidence from clinical and genomic features. J Clin Oncol. 2011; 29(11):1415–1423. [PubMed: 21357789]

25. Taylor MD, Northcott PA, Korshunov A, Remke M, Cho YJ, et al. Molecular subgroups of medulloblastoma: the current consensus. Acta Neuropathol. 2012; 123(4):465–472. [PubMed: 22134537]
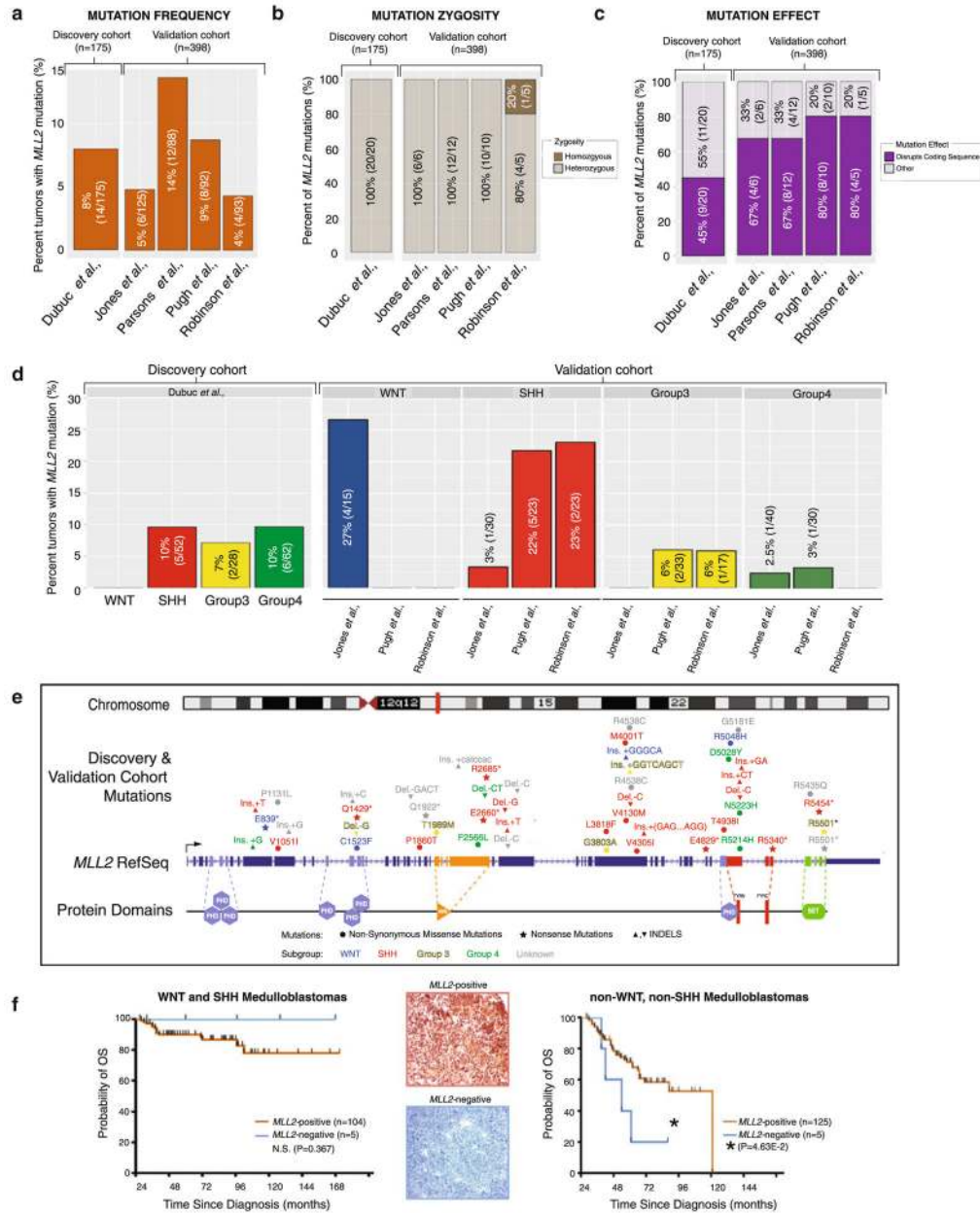
Fig. 1.
MLL2 mutations in medulloblastoma are independent of molecular subgroup and lack prognostic utility. **a** Incidence of *MLL2* mutations across a discovery (*n* = 175) (*left*) and validation cohort (*n* = 398) (*right*). **b** Percent distribution of *MLL2* homozygous versus heterozygous mutations based on allele frequency, identifies a single homozygous mutation (1/53) across the combined cohorts. **c** Analysis of the functional consequences of *MLL2* mutations highlights a significant fraction of discovery (45 %) and validation (67–80 %) single nucleotide variants that disrupt the *MLL2* coding sequence through frameshift and nonsense mutations ablating enzymatic methyltransferase activity. **d** Subgroup-specific examination of *MLL2* mutations describes the extensive variability across both sequencing cohorts suggesting *MLL2* mutations occur independent of molecular subgroup. **e** Schematic representation of the *MLL2* mutational landscape in medulloblastoma indicates single

nucleotide variants scattered throughout the coding sequence and the absence of a mutational hotspot. A single recurrent mutation (R5501*) was identified across 53 *MLL2* mutations. **f** *MLL2* immunohistochemical (IHC) analysis provides no prognostic utility based on presence/absence of MLL2 protein expression for WNT and SHH subgroups (*left*), whereas loss of MLL2 protein expression was significantly ($P < 4.63E–2$) associated with survival for Group 3 and Group 4 (i.e., non-WNT, non-SHH) tumors (*right*)
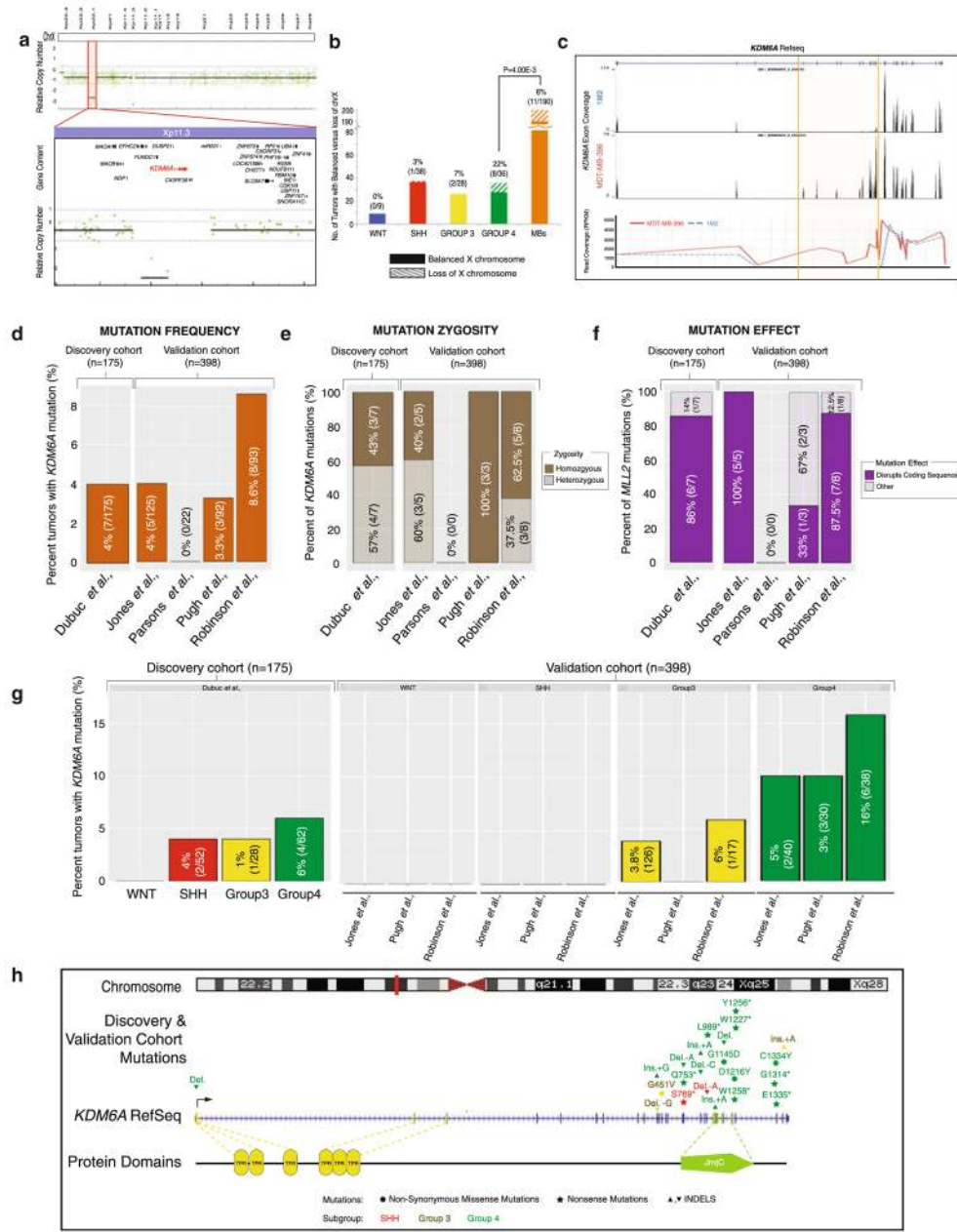
Fig. 2.

Identification of focal deletions of *KDM6A*, and mutations that are enriched in Group 4 tumors. **a** Analysis of medulloblastoma copy number aberrations reveals one (0.5 %, 1/203) tumor with a homozygous deletion spanning *KDM6A*. **b** Subgroup-specific distribution of X-chromosome loss across 190 primary medulloblastomas studied by Affymetrix 500 K SNP arrays demonstrates a significant ($P = 4.00E-3$) enrichment of this cytogenetic event in Group 4 medulloblastomas (22 %, 8/36). **c** Targeted exon-capture and sequencing identifies a medulloblastoma (0.6 %, 1/175, 1M2) with a *KDM6A* intragenic deletion spanning exons 5 through 13. **d** Frequency and percent of *KDM6A* mutations across a discovery cohort of 175 primary tumors (*left*) and a validation cohort of 398 tumors (*right*) reveals mutations in 4–8 % of tumors. **e** Allele frequency inference of *KDM6A* mutation zygosity highlights the abundance of homozygous mutations across both cohorts. **f** Percent distribution of *KDM6A*

mutations which disrupt the coding sequence (frameshift or nonsense mutations) versus non-disruptive nucleotide changes (missense and in-frame INDELs) accents the frequent disruptive nature of *KDM6A* mutations across the discovery and validation cohorts. **g** Subgroup-association of *KDM6A* mutations demonstrates predominant targeting of Group 4 medulloblastomas. **h** Mutational landscape of KDM6A across 573 tumors (combined discovery and validation cohort) calls attention to the 3′ localized, damaging and Group 4-enriched nature of *KDM6A* single nucleotide variants
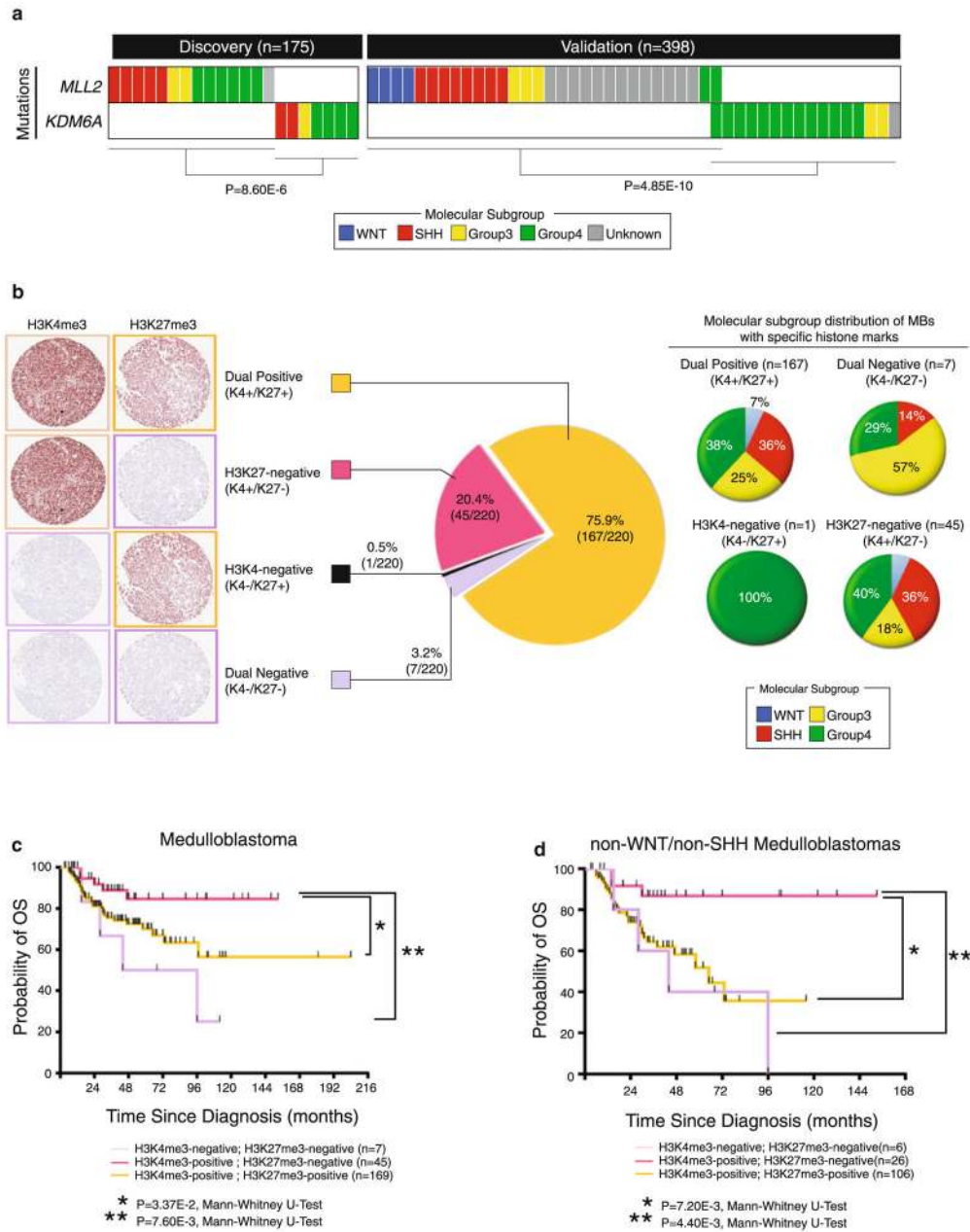
Fig. 3.
H3K4me3 and H3K27me3 staining reveals deregulation of the histone code in a significant fraction of medulloblastomas. **a** Analysis of *MLL2* and *KDM6A* mutations demonstrates the mutually exclusivity ($P = 8.60E–6$) and mutational inactivation of chromatin-modifier genes in 12 % (21/175) of the discover cohort. The validation cohort recapitulated these findings ($P = 4.85E–10$); however, a single tumor was identified with both *MLL2* and *KDM6A* mutations. Importantly, the *MLL2* mutation in this case was a missense variant with no known deleterious effect to protein functionality. **b** H3K4me3 (K4) and H3K27me3 (K27) immunostaining results identifies populations of medulloblastomas with modifications from the expected (K4+/K27+) staining patterns in 23.5 % (53/222) of tumors analyzed, suggesting deregulation of the histone code is a common occurrence in medulloblastoma (*left*). The molecular distribution of medulloblastomas with specific histone marks (*right*). **c**

Survival analysis of medulloblastomas with normal (K4+/K27+) or aberrant (K4+/K27−; K4−/K27+; K4−/K27−) histone code demonstrates distinct clinical differences with improved outcome associated with K4+/K27− and dismal outcome associated with dual negativity (K4−/K27). **d** Subgroup-specific analysis of chromatin marks demonstrates the clinical significance associated with H3K4me3 and H3K27me3 staining patterns are driven by Group 3 and Group 4 medulloblastomas
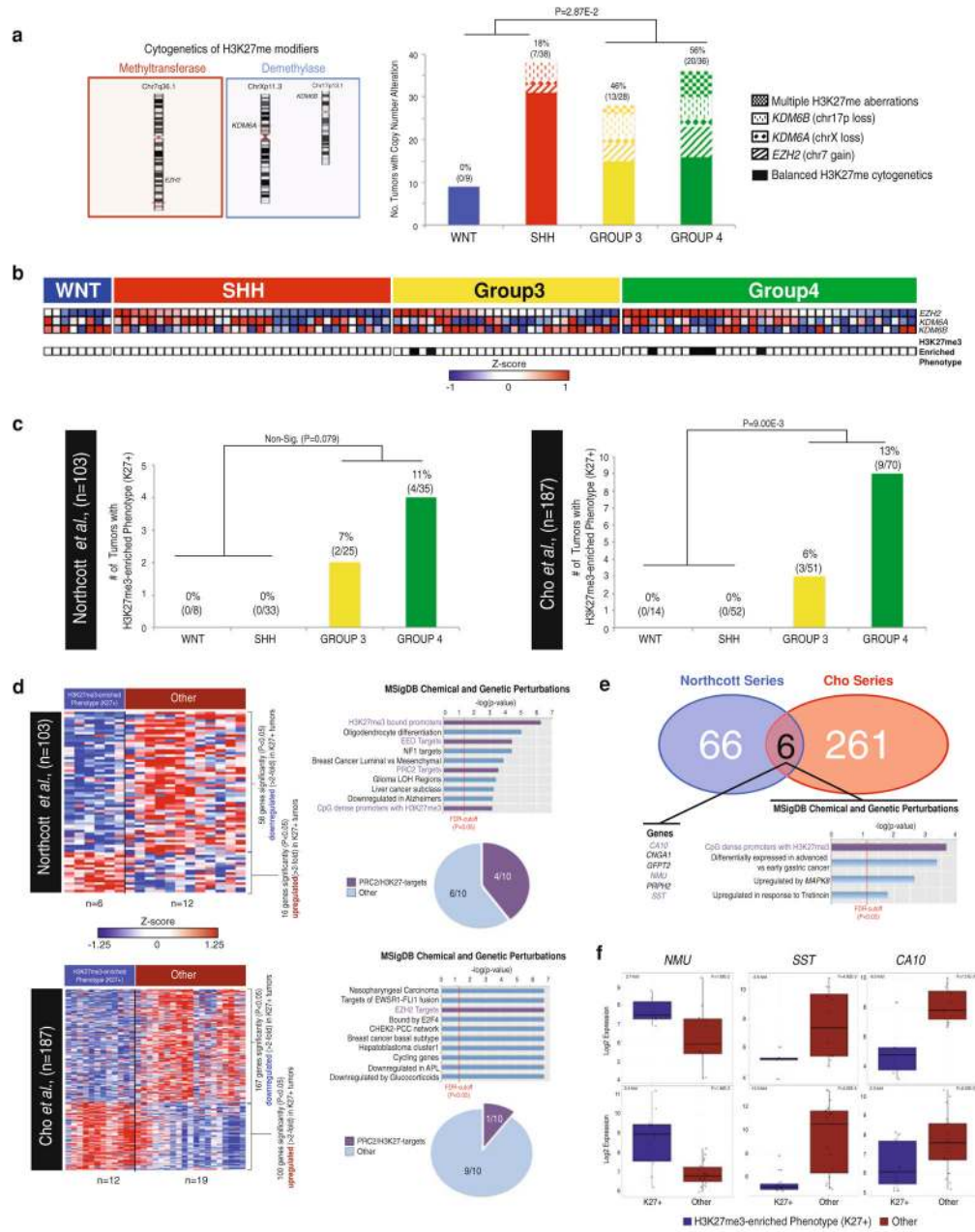
Fig. 4.
Identification of a genomic and transcriptional H3K27me3-enrichment phenotype (K27+) in Group 4 medulloblastomas. **a** Cytogenetic distribution of H3K27me methyltransferases (*EZH2*, chr7q36.1) and demethylases (*KDM6A*, chrXp11.3; *KDM6B* chr17p13.1) (*left*) and a subgroup-specific analysis of cytogenetic aberrations resulting in the accumulation of H3K27me3 identifies a significant (*P* = 2.87E−2) enrichment in Group 3 and Group 4 medulloblastomas versus WNT and SHH tumors (*right*). **b** Over-expression of H3K27-methyltransferases and down-regulation of H3K27-demethylases reveals a H3K27-methylator phenotype (K27+) occurring exclusively in Group 3 and Group 4 medulloblastomas across 103 primary medulloblastomas. **c** Discovery and validation transcriptome cohorts comprising 290 tumors demonstrate a statistically significant

enrichment of an H3K27-methylator phenotype (K27+) in Group 3 and Group 4 MB. **d** Transcriptome-wide analysis of significantly ($P < 0.05$) and differentially (>2-fold) expressed genes in H3K27-methylator phenotype (K27+) versus non-K27+ medulloblastomas. Molecular Signature (MSigDB) analysis reveals extensive deregulation of PRC2-target genes in the discovery (40 %) and validation (10 %) cohorts. **e** Comparison of significantly ($P < 0.05$) and differentially (>2-fold) expressed genes across the discovery and validation transcriptome cohort reveals a small number of overlapping genes. Many of the overlapping genes (50 %, 3/5) have previously been implicated as H3K27me3-targets. **f** Dot plot analysis of genes putatively regulated by H3K27me3 methylation across both the discovery and validation transcriptome cohorts highlights the significantly differential fold changes and possible utility for future PRC2-therapy-related diagnostics
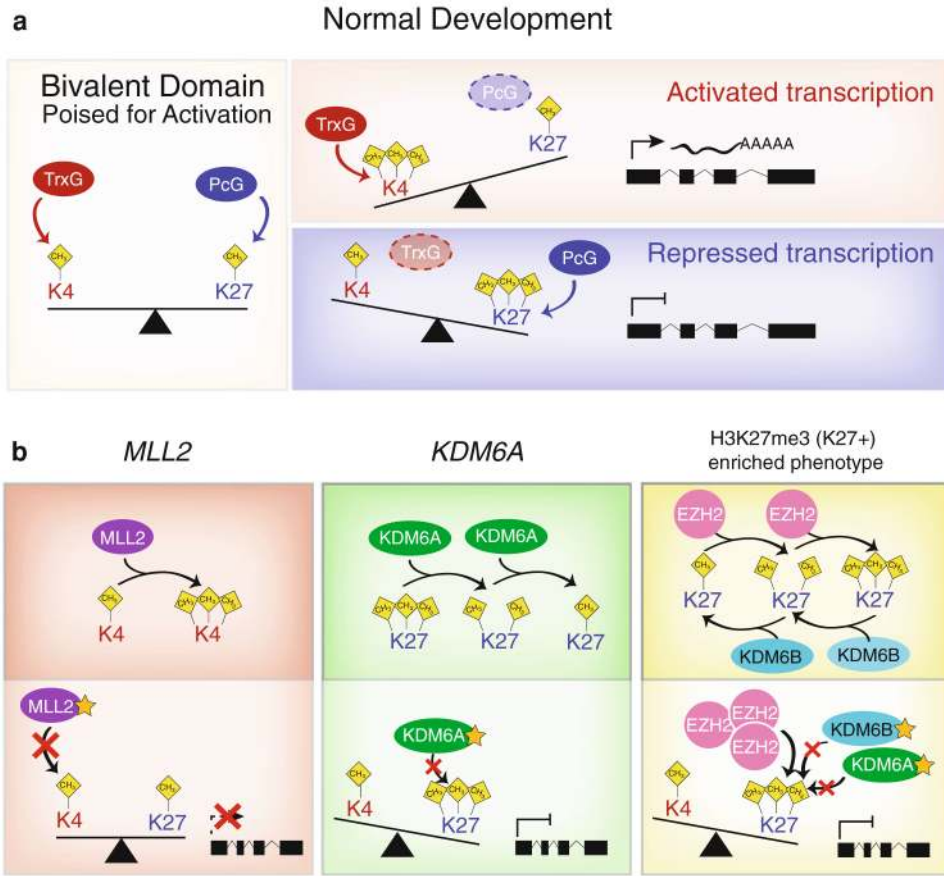
Fig. 5.
Schematic representation of normal developmental Trithorax (trxG) and Polycomb (PcG) group proteins and the effects of *MLL2* and *KDM6A* mutations on chromatin state and transcriptional activation. **a** Representation of the balancing act of bivalent domains in which Trithorax (trxG) and Polycomb (PcG) group proteins counteract each other to maintain genes poised for activation. Activation of gene expression through a trxG-mediated shift towards H3K4-trimethylation and repressed transcription via PcG-regulated H3K27me3 induce differentiation. **b** Wild-type and pathogenic roles of *MLL2* and *KDM6A* on chromatin state and transcription. *MLL2* functions as H3K4 methyltransferase shunting promoters towards an active state. *MLL2* mutations in medulloblastoma largely disrupt the coding sequence through nonsense and frameshift mutations causing premature truncation of the transcript and ablation of the methyltransferase activity preventing the normal activation of gene expression. KDM6A, a H3K27-demethylase, functions as a trxG-protein to inhibit PcG-mediate H3K27me3 marks. *KDM6A* mutations in medulloblastomas result in the accumulation of H3K27me3, normally removed by the wild-type gene. In Group 3 and 4 medulloblastomas an H3K27me3-enriched phenotype (K27+) is observed, in which overexpression of the H3K27-methyltransferase *EZH2* with concomitant down-regulation of both *KDM6A* and *KDM6B* demethylases results in a strong shift towards increased H3K27me3